LUND
UNIVERSITY

Simulations of polymer solutions displaying a lower critical solution temperature

Sandra M. Larsson

Bachelor of Science Thesis, 30 hp

August 29, 2018

Department of Chemistry

Division of Theoretical Chemistry

Supervisor: Jan Forsman

Examiner: Per-Olof Widmark

Abstract

Thermoresponsive polymers with a lower critical solution temperature, LCST, have attracted interest in the development of new "smart materials", which change properties in response to external stimuli. Polymers with an LCST near physiological temperatures are especially relevant in biomedical applications, most notably perhaps in drug delivery systems.

The aim of this work is to investigate polymer solutions with an LCST using a coarse-grained model where the monomers of the polymer chains exist in one of two states; one solvophilic and one solvophobic state, where the degeneracy of the solvophobic state is higher than that of the solvophilic. Metropolis Monte Carlo simulations were performed on both single-chain and multiple-chain systems, and on chain-lengths varying between 20 and 400 monomers. Simulations on single-chain systems showed a collapse for chains with 40 or more monomers, while the investigated multiple-chain systems of all chain-lengths aggregated. Due to fluctuations in the temperature at which the collapse occurred, as well as inconsistencies between simulations performed by decreasing and increasing the temperature, further investigations are needed to determine the limitations of the model and its usefulness in describing polymer solution behaviour.

Populärvetenskaplig sammanfattning

Polymerer är långa kedjor av upprepade segment och finns både som naturliga polymerer (proteiner, DNA, gummi, och cellulosa) och som syntetiskt fram-ställda polymerer (plaster, nylon, etc.). Många polymerer är känsliga för ändringar i deras miljö och termoresponsiva polymerer, som har studerats i detta arbete, ändrar egenskaper drastiskt vid ändringar i temperaturen. Vid en viss kritisk temperatur, som är specifik för den enskilda polymeren, går dessa polymerer från att vara utsträckta kedjor, lösliga i medlet de befinner sig i, till att kollapsa och bilda tätpackade kluster som kan fällas ut från lösningen.

Termoresponsiva polymerer är intressanta att studera på grund av deras applikationer som "smarta material". De kan till exempel användas inom transportsystem för läkemedel som en del av läkemedelskapseln, då de skulle kunna reagera på temperaturen i omgivningen för att veta när kapseln har kommit rätt och frisätta läkemedlet på en lämplig plats i kroppen.

Datorsimuleringar av dessa typer av polymerer kan ge en större inblick i hur och varför polymererna kollapsar, samt hur olika egenskaper av polymeren och hur yttre faktorer påverkar temperaturen polymererna kollapsar vid. Simuleringar av större polymersystem, med många och långa kedjor är mycket tidskrävande och det är därför önskvärt att kunna beskriva polymerernas beteenden vid olika temperaturer med en enklare modell. I detta arbete har därför en enklare modell användts för att studera polymerlösningar. Både enstaka polymerer och större system med flera polymerkedjor har studerats och det har undersökts om det går att se en direkt koppling mellan kollapsen av en kedja och aggregeringen av ett helt system till ett hoppackat kluster. Simuleringarna har visat att modellen kan beskriva den plötsliga kollaps av polymerer som sker vid en viss temperatur både för enstaka polymerer och för flera polymerer. Det fanns dock en variation i när denna kollaps skedde för båda systemen och därför kunde inte en specifik temperatur för aggregeringen bestämmas. Det fanns även stora skillnader i förhållandena vid vilka en kollaps kunde ses för simuleringar där temperaturen ökades jämfört med sänktes. Detta är något som hade behövt undersökas nogrannare för att ta reda på modellens begränsningar i att beskriva det undersökta fenomenet.

Contents

1 Introduction

Thermoresponsive polymers with a lower critical solution temperature, LCST, exhibit an often drastic change in miscibility in response to a change in temperature through a critical temperature.[1] Below the LCST a polymer solution is completely miscible at all concentrations. As the temperature is increased to above the LCST, the system separates into two phases, one enriched in polymer and one depleted of polymer. This phase separation is accompanied by a change in the conformation of the polymer from an expanded coil to a collapsed globule.[2] Due to their drastic change in miscibility in response to external stimuli, thermoresponsive polymers have attracted interest in the development of new "smart materials". In particular, polymer solutions with an LCST around physiological temperatures have found applications in areas such as drug delivery systems[3,4,5] and tissue engineering[6,7,8].

Polymer solutions with an LCST have been studied with computer simulations in a number of papers before[9,10,11], and recently aggregation of PNnPAm (poly(*N*-*n*-propylacrylamide)) chains above the LCST for systems with multiple chains using full-atom molecular dynamics simulations was reported by de Oliveira et al.[12] However, due to the computational power required to simulate systems of multiple polymer chains with more complicated models, systems with a larger number of chains, and with longer polymer chains, are difficult subjects for theoretical studies.

In this work, a simple model of a polymer solution, originally developed by Karlström[13] to explain the LCST displayed by the poly(ethylen oxide)-water system is used to study polymer solutions with an LCST. The model is coarse-grained and allows the monomer segments to occupy two states, one solvophilic and one solvophobic. The degeneracy of the solvophobic state is higher, thus inducing the monomers to populate the solvophobic state at higher temperatures. The aim of the project is to investigate whether the model can be used to explain the coil-to-globule transition that occurs above the LCST using both single- and multiple-chain Monte Carlo simulations. The connection between the collapse of a single chain and the aggregation of a multiple-chain system will also be explored.

2 Polymer solutions and simulation theory

2.1 Polymer solutions and critical solution temperatures

The quality of the solvent of a polymer-solvent system determines the conformation of the polymers in the solution. In a good solvent, polymers adopt an extended coil conformation to maximize the favourable interactions with the solvent molecules. In a bad solvent, the polymer tends towards minimizing interactions with the solvent, thus folding in on itself and adopting a more compact globule

conformation. As the quality of the solvent and its interactions with the polymer changes with temperature, so the conformation of the polymer changes. This is commonly known as the coil-globule transition and occurs when the solvent quality goes from good to bad and the previously expanded coil collapses to form a globule.[2] When this collapse occurs as the temperature is dropped, the polymers are said to have an upper critical solution temperature, UCST. When the same happens as the temperature is increased, the polymer instead has a lower critical solution temperature. At temperatures above the UCST or below the LCST, the system is completely miscible at all polymer concentrations. In the phase diagram of temperature as a function of composition for a polymer with a UCST or LCST, see figure 1, the area enclosed by the curves marks the region where the polymer collapses and the system separates into two phases.[14]

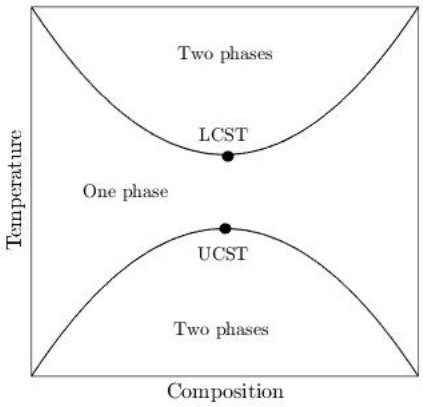

Figure 1: The phase diagram for a polymer with an LCST and a UCST. The area above the upper curve and below the lower curve marks the two-phase region.

A lower critical solution temperature often occurs in systems where there is extensive hydrogen bonding between the polymer and the solvent. As the temperature increases, the highly directional hydrogen bonds in such a system are disrupted due to the increased thermal motion of the molecules. The decrease in favourable polymer-solvent interactions causes the phase separation observed in solutions with an LCST.[2]

2.2 Measuring polymer size

The size of a polymer can be measured in many ways. Two of the most common methods to measure the size is the root-mean-square end-to-end distance and the root-mean-square radius of gyration. The end-to-end distance is the separation between the two ends of a polymer. The radius of gyration, R_g^2, is the average distance of the monomers of a polymer from the centre of mass of the entire coil

or the mean position of the monomers and can be calculated accordingly:[2]

$$R_g^2 = \frac{1}{N} \sum_{i=1}^{N} (\vec{r}_i - \vec{r}_{mean})^2 \tag{1}$$

where N is the number of monomers in the polymer, $\vec{r}_i$ is the position vector of each monomer and $\vec{r}_{mean}$ is the mean position vector of all monomers in the coil.[15]

2.3 The Monte Carlo method

The two most common methods when simulating molecular systems are molecular dynamics, MD, and the Monte Carlo method, MC.[15] While molecular dynamics simulates the movements of atoms and molecules, Monte Carlo generates configurations from which equilibrium thermodynamic properties can be calculated.[2,14] The crude Monte Carlo method is performed by generating random coordinates for all particles in the system. This is repeated so that multiple configurations of the system are obtained. The average of a thermodynamic property is then calculated by performing a summation over all configurations and weighing each individual value of the property with the Boltzmann factor ($\exp\left(\frac{-E}{k_B T}\right)$, where E is energy, k_B is the Boltzmann constant and T is the absolute temperature) of the energy of the system at that configuration:[14]

$$X_{avg} = \sum_{i=1}^{N} P_i \cdot X_i \tag{2}$$

where X is an arbitrary property, N is the number of configurations and P is the probability of the configuration and is calculated from the Boltzmann factor.[14]

However, for many configurations the Boltzmann factor and thus the probability of the configuration will be very low due to overlap between the particles. These configurations will then have a low contribution to the average of the property and it will be time-consuming to count these configurations. The Metropolis Monte Carlo method improves on the efficiency of the algorithm by only counting more probable contributions to the average.[14]

2.3.1 The Metropolis Monte Carlo method

In the Metropolis Monte Carlo method, an initial configuration of the system is generated, whereby a random particle is chosen and undergoes a trial displacement. The change in energy for the system after the displacement is calculated, and the displacement is allowed and kept if the Boltzmann factor for the energy change is larger than a random number between 0 and 1. This means that all moves which

lead to a negative energy change (a decrease in energy for the new system) are allowed. Displacements leading to a positive change in energy however, are allowed with a probability equal to the Boltzmann factor of the energy change. Then for each configuration, whether a displacement was accepted or not, the measured property is calculated and each contribution to the average of the property is weighted equally.[16]

2.4 Intermolecular interactions

The interaction between neutral atoms or molecules can be described with various models differing in simplicity and accuracy. A simple model of the pairwise potential between atoms is the hard-sphere potential, see figure 2a. The potential is infinitely large at separations smaller than a parameter σ (usually taken as the diameter of the particle) and zero at all separations larger than or equal to σ. The hard-sphere model only takes into account the repulsion between atoms resulting from overlapping electron orbitals. Attractive interactions between neutral molecules can be included by expanding the hard-sphere model to a square-well model (see figure 2b), which is identical to the hard-sphere potential except for a potential well at separations between σ and a cut-off distance larger than σ.[17]

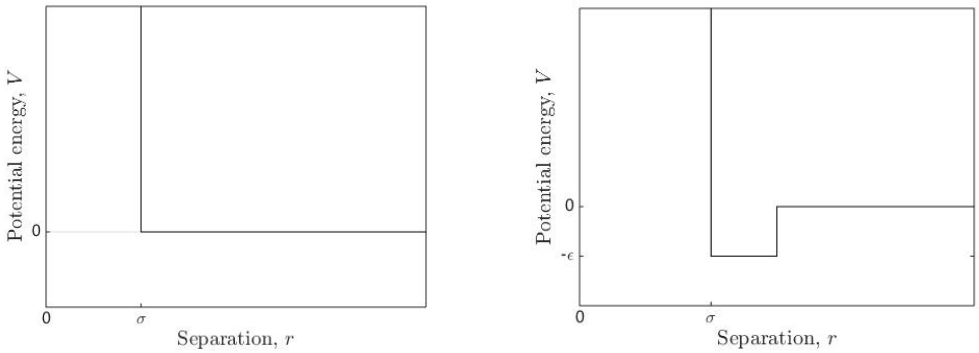

(a) **(b)**

Figure 2: The hard-sphere (a) and square-well (b) potentials, V, as functions of particle separation, r.

The square-well potential is still quite a crude approximation of the real interaction potential for most systems. A more accurate representation of the potential between neutral atoms is the Lennard-Jones potential (see figure 3):[14]

$$V = 4\varepsilon \left[\left(\frac{\sigma}{r} \right)^{12} - \left(\frac{\sigma}{r} \right)^{6} \right] \tag{3}$$

where V is the potential, ε is the depth of the potential well, σ is the point where the potential goes *through* zero and r is the separation between the particles.[14]

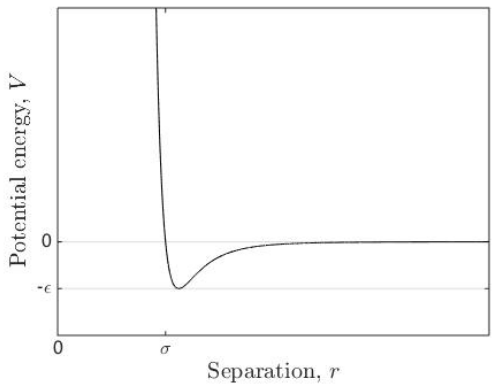

Figure 3: The Lennard-Jones potential, V, as a function of particle separation, r.

2.5 Periodic boundary conditions

Samples of bulk liquids contain a very large number of molecules. Due to the computing time required to simulate such large systems, it is more convenient to represent the bulk system with a smaller number of molecules contained within a simulation box. However, in a smaller system the disparity between the net forces on the molecules near the walls and at the centre of the box leads to a poor representation of the bulk material, where the distance to the walls is large enough for the interfacial forces to be insignificant. The effect of the walls on the intermolecular interactions is usually circumvented by using periodic boundary conditions. Here, the walls of the box is thought of as being continuous, so that a particle leaving the box on one side will re-enter the box from the opposite side. Thus, particles close to one side of the box will be neighbours to the particles close to the opposite side of the box.[17]

3 Simulation model and methods

The thermoresponsive behaviour of neutral polymers was investigated with Metropolis Monte Carlo simulations. These were performed on polymer systems both with a single polymer chain and on systems with multiple chains. The polymers both in the single-polymer simulations and the multiple-polymer simulations were represented with the same model.

3.1 Polymer model

The monomers in the polymer chains were modelled as beads connected to each other with a fixed bond length where the bond angles were fully flexible. The

model used for the interactions between the monomers was originally developed by Karlström[13] and later adopted in a density functional treatment by by Xie et al.[18,19,20]. Here the monomers are able to switch between two classes of states, A and B, where B states are more hydrophobic than A states. The degeneracy of a B state is higher than an A state, which means that at higher temperatures, more of the monomers will switch to a B state and the hydrophobicity of the polymer as a whole will increase. However, the B states are higher in energy than the A states. The two classes of states are meant to represent the monomers being able to switch between conformations with different intrinsic polarities (such as trans and gauche conformations). The increased hydrophobicity of the polymers as the temperature is raised mimics the disruption of hydrogen bonding between the solvent and the polymer which occurs at higher temperatures.

3.2 Simulation methods

The monomers in the hydrophilic state A were modelled as hard spheres. The monomers in a B state were also modelled as hard spheres, but with an added Lennard-Jones potential at distances larger than a parameter σ. A cut-off distance was introduced to the Lennard-Jones potential to improve computing efficiency. The B state was also given an energy penalty to be overcome at switches between A and B states. The initial conformations of the polymers were generated by a random growth of the polymer chain where overlap between monomers was disallowed. For the multiple-chain simulations the first monomer in each chain was generated at a random starting position in the simulation box, and then the rest of the chain was generated in the same fashion as the single chains.

For the single polymer simulations, no simulation box was used and the polymer was allowed to move in free space. Three types of moves were used; pivot moves, where a segment of the chain is rotated while the rest of the chain stays fixed, crankshaft moves, where a single monomer is rotated around the axis created by its two neighbours while maintaining correct bond lengths, reptation moves, where one of the monomers at the ends of the chains is moved to a random position at the other end of the chain, and switches between the two monomer states A and B.

In the multiple polymer simulations, periodic boundary conditions in a simulation box of a fixed volume and number of chains were used. Here, six types of moves were used in the simulations; the four moves used in the single-chain simulations (pivot moves, crankshaft moves, reptation moves and state switches), as well as translational and rotational moves of the entire polymer chain.

3.3 Simulation details

Both single chain and multiple chain simulations were performed on polymers of lengths 20, 40, 60, 80, 100, 150, 200, 300 and 400 monomers. Simulations were performed both with increasing and decreasing temperatures, all with a step size of 20 K, as well as simulations on single, fixed temperatures. An equilibration run of between 20 and 50 % of the length of the production run was performed before each new measurement or adjustment of the temperature.

Whereas the degeneracy of class A was kept constant at one in all simulations, runs with varying degeneracies of class B were performed. Three different degeneracies were tested; 24, 36, and 72. All other simulations were performed with a B-degeneracy of 36. The parameter σ was kept at 0.65 bond lengths and the cut-off distance for the Lennard-Jones potential was kept at 5 bond lengths for most simulations. The penalty for the B states was 1200 k_B and epsilon was 150 k_B throughout most of the simulations. A cut-off distance of 2 bond lengths and energy penalties for the B states of 1250 to 1500 k_B was tried for some of the single chain simulations.

4 Results and discussion

4.1 Single-chain simulations

4.1.1 The radius of gyration during runs with increasing and decreasing temperatures

Simulations on single polymer chains of 40 monomers and larger all showed a structural transition from an expanded coil conformation to a collapsed globule upon increasing the temperature of the system. A plot of the average gyration radii during a production run at temperatures increasing from 20 K can be seen in figure 4a for polymers of 20, 40 and 60 monomers. For the 40 and 60 monomer chains, a sudden drop in the radius of gyration can be seen at 200 to 220 K for the 60-mer and at 180 to 200 K for the 40-mer chains. This drastic decrease in the radius of gyration indicates a phase transition of the system. As the temperature is increased further, the radius of gyration of the collapsed 40- and 60-mers rises and the collapsed globule expands to adopt a coil conformation again. For the 40-mer, the radius of gyration increases rapidly after the transition temperature until around 260 K after which the graph levels off, while for the 60-mer, the unfolding of the chain is much slower.

The simulations on a polymer consisting of 20 monomers showed that the radius of gyration of the polymer fluctuated around a relatively constant value with no

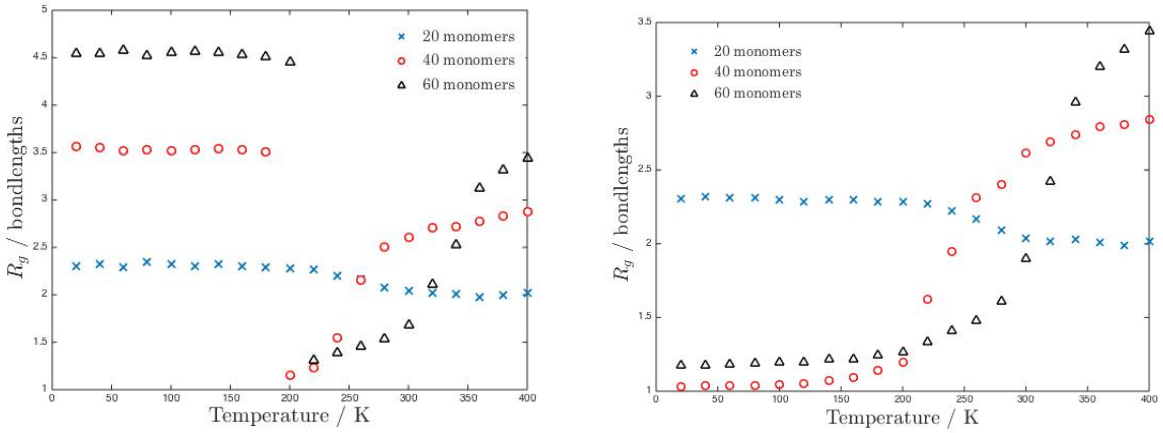

(a) **(b)**

Figure 4: The average radius of gyration during a production run for polymers of 20, 40 and 60 monomers for increasing (a) and decreasing (b) temperatures.

sudden drop in the radius of gyration. It is therefore likely that the limiting polymer length to observe a phase transition using this model is 20 monomers for single-chain simulations.

When performing the same simulations, but instead decreasing the temperature of the system, the previously observed phase transition disappears. Figure 4b shows a plot of the average radius of gyration during a production run for polymers of 20, 40 and 60 monomers where the temperature is decreased from 400 K. For the 20-mer, for which no phase transition was observed, the values for the radius of gyration for the run where the temperature is increased, and for the run where the temperature is decreased are strikingly similar. The same is true for the 40-mer and the 60-mer at temperatures above the phase transition. However, at temperatures below where the phase transition was observed, no drastic increase in the radius of gyration is observed and no unfolding of the chain occurs. Instead, the radius of gyration continues to decrease slightly.

4.1.2 Runs with longer polymer chains

Simulation runs with longer polymer chains consisting of 100 to 400 monomers showed signs of a lower critical solution behaviour when the temperature was increased, but not on runs where the temperature was decreased, in accordance with the results from simulations with shorter polymer chains. Figure 5 shows a plot of the radius of gyration at temperatures between 20 and 400 K for 100, 200, 300 and 400 monomer chains during simulation runs where the temperature was increased in 20 K steps. It can be seen that there is a large drop in the radius of gyration for all chain lengths between the temperatures 180 and 200 K. The plot

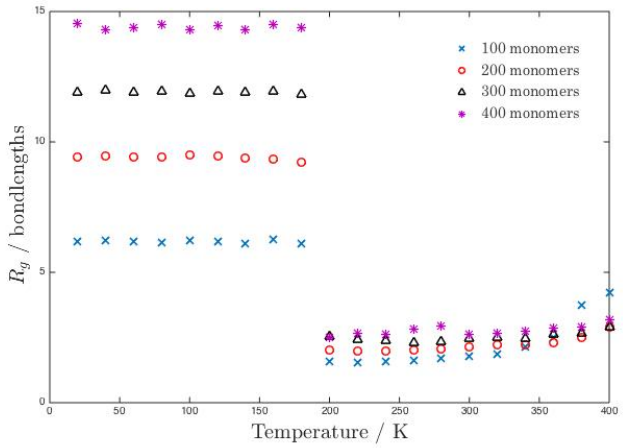

Figure 5: The average radius of gyration during a production run for polymers with 100, 200, 300 and 400 monomers for increasing temperatures.

shows that at temperatures after the drop, the radius of gyration does not increase as quickly for longer chains as for shorter. Only the 100-mer unfolds significantly, and not as much as the 40 or 60-mer chains in figure 4a. Since it is possible that the longer chains have more difficulties in unpacking due to being more entangled than the shorter chains, it cannot be said for certain that this is an actual trend.

4.1.3 Visual confirmation of chain collapse

The coil-globule transition was also observed in snapshots of the polymer chains during the simulations where the temperature was increased in steps. Figure 6a shows a 40 monomer polymer as an expanded coil at a temperature of 180 K, just before the phase transition as seen in figure 4a, and figure 6b shows the same polymer as a collapsed globule at a temperature of 200 K. Snapshots from simulations on polymers with more than 40 monomers also confirmed a similar collapse. Another example is shown in figure 6c and 6d for a polymer with 200 monomers. Snapshots of the 20-mer showed that the polymer adopted an expanded coil structure at all investigated temperatures, so no phase transition was observed for a chain-length of 20 monomers.

4.1.4 The ratio of B monomers

A plot of the average ratio of B monomers during a production run for the polymers of chain-length 20, 40 and 60 monomers at increasing temperatures can be seen in figure 7a. For all chain lengths, almost no monomers occupied the solvophobic B state at lower temperatures. At higher temperatures, the B state was considerably

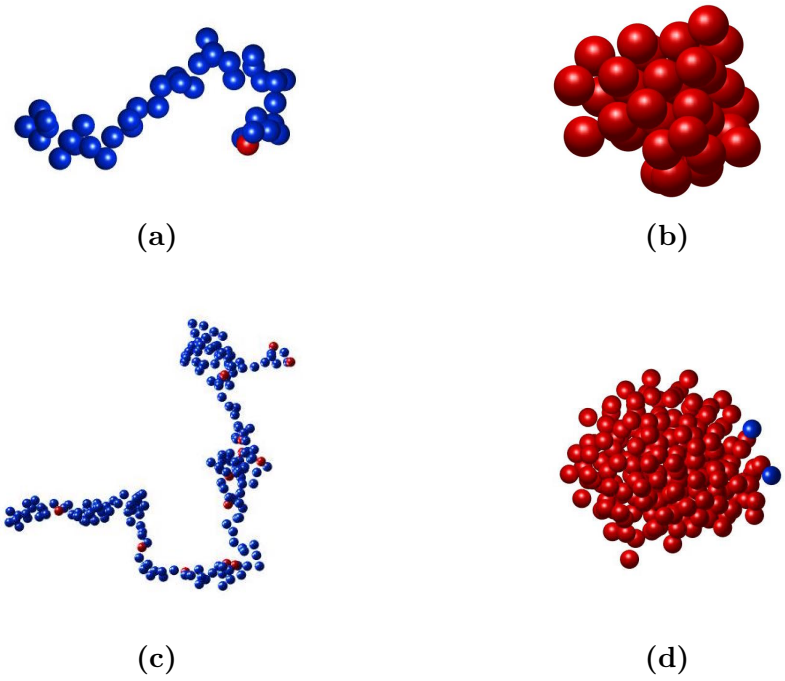

Figure 6: Simulated polymer chain of 40 (a,b) and 200 (c,d) monomers as a coil before the phase transition (a,c) and as a globule after the phase transition (b,d). The monomers are modelled as spheres where the blue monomers are in state A and the red monomers are in state B.

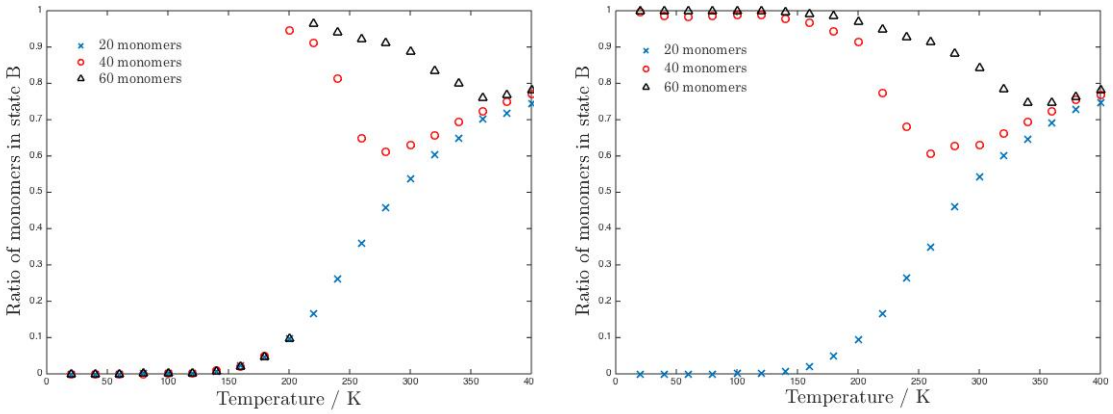

(a) **(b)**

Figure 7: The average ratio of B monomers during a production run for polymers of 20, 40 and 60 monomers for increasing (a) and decreasing (b) temperatures.

more populated than state A. It can also be seen in figure 7a that for the 20 monomer chain, which did not undergo a phase transition, the graph of the B state ratio as a function of temperature seems to be S-shaped. For the 40 and 60 monomer chains that did go through a phase transition, it can be seen that almost all monomers suddenly switch from state A to state B at the temperature at which the phase transition occurs, whereas they at even higher temperatures seem to all go towards the same ratio of B state monomers as the 20-monomer chain.

In figure 7b a plot of the average ratio of B monomers during a production run for 20-, 40- and 60-monomer chains at decreasing temperatures can be seen. Here, as with the plots for the radius of gyration at increasing and decreasing temperatures, values for the B ratio at temperatures higher than the temperatures at which the collapse of the chains were observed, took on almost the same values in both simulation runs. However, at lower temperatures the ratio of B monomers in figure 7b continued at ratios close to one for the 40- and 60-mers and did not drop to a lower value. This is consistent with the plots of the radius of gyration for the same chains. For the 20-monomer chain, the two graphs looked almost identical.

4.1.5 Inconsistencied in the temperature of collapse

When adjusting the simulation time of the runs with increasing temperatures, it was observed that the longer the simulation time, the lower the temperature at which the collapse occurred. Figure 8 shows a plot of the radius of gyration at temperatures between 20 and 300 K for a 100-mer during increasingly longer simulations. It can be seen that the collapse occurs at lower and lower temperatures for the long runs. Curiously, it was also observed that for the very long runs, the

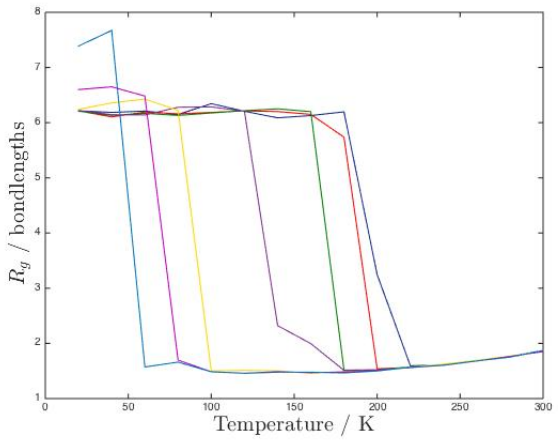

Figure 8: The radius of gyration for a 100-mer at temperatures between 20 and 300 K at intervals of 20 K performed for increasingly longer runs. The lines which show drops in R_g at lower temperatures are runs performed with longer simulation times.

radius of gyration at the expanded state was significantly higher than for shorter and mid-range simulation times.

To further investigate this phenomenon, runs at fixed temperatures were performed and the value for the radius of gyration as a function of trial Monte Carlo moves was plotted for temperatures between 20 and 600 K in steps of 20 K. Figure 9 shows four such plots at temperatures of 100, 200, 220 and 240 K for a chain with 100 monomers. It was seen that for temperatures of 220 K and above the radius of gyration almost immediately dropped to the equilibrium value, where it stayed constant with some variations during the entire run. For 200 K and all the way down to 60 K, the radius of gyration initially stayed at what seemed to be a mostly constant value with no trends of decreasing, until the chain suddenly collapsed during the course of a relatively small number of trial moves. For 20 and 40 K, no collapse could be observed, but it is likely that given even longer simulation times, the chains would have collapsed.

Looking at the energetics of the collapsed and expanded chain states for the lower temperatures in runs of decreasing and increasing temperatures, it could be seen that while the coil state at temperatures between 1 and 160 K was around zero, the globule state at the same temperatures were large negative values close to 0 K and smaller negative values for the higher temperatures in the same range. So while the globule state is much lower in energy than the coil state, it is possible that some kind of energy barrier exists that makes it difficult for the coil state to collapse at the lower temperatures.

Simulations were also performed with an increased energy penalty for B states, and with different values on parameters for the cut-off distance of the Lennard-

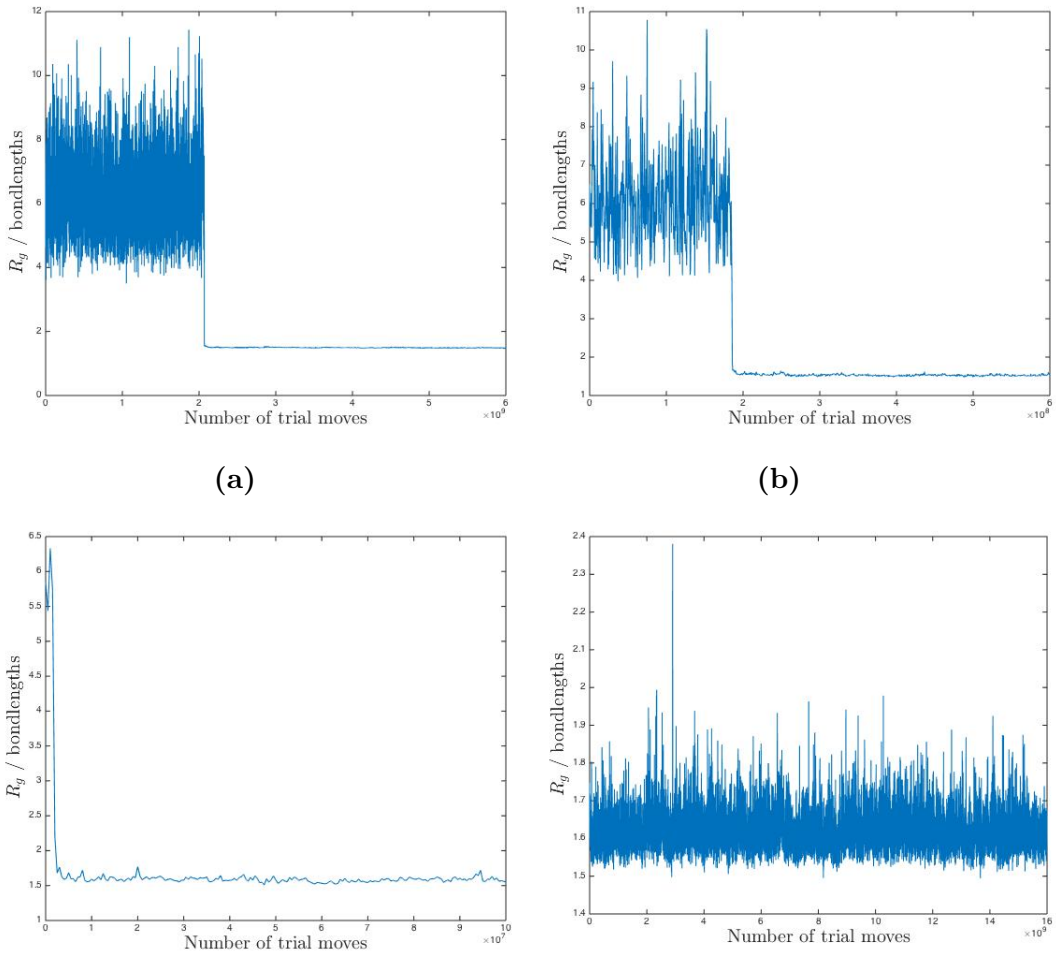

Figure 9: The radius of gyration of a 100-mer chain as a function of the number of Monte Carlo trial moves for temperatures of 100 (a), 200 (b), 220 (c) and 240 (d) K.

Jones potential. During simulations where the energy penalty for B states was increased, a phase transition during decreasing temperature runs was observed, however, at the same conditions, the phase transition during increasing temperatures disappeared. After adjusting the parameters, signs of a phase transition appeared on both increasing and decreasing runs, however, the phase transition was not as clear cut as for some of the other simulations.

It could be that these discrepancies are due to another phase transition from an upper critical solution temperature existing in the same temperature range as the LCST. But further investigations are needed to determine the exact nature of this relationship.

4.1.6 Varying the degeneracy of the B state

The simulations with different degeneracies of the B state showed that the degeneracy affected both the temperature at which the the coil-to-globule transition occurred as well as how quickly the globule unfolded at higher temperatures. A plot of the average radius of gyration as a function of temperature for the three investigated degeneracies of the B state can be seen in figure 10. It can be seen in the graph that the collapse of the polymer chain occurred earliest for the simulation with a B state degeneracy of 72, at around 160 K, while for a degeneracy of 36 the collapse occurred at 220 K. The subsequent unfolding of the polymer chain after the initial collapse could also be seen to become increasingly outstretched over a large temperature range for increasing degeneracies of state B.

However, for a B state degeneracy of 24, no collapse of the polymer chain was observed. In figure 10 it can be seen that the radius of gyration slowly starts to decrease after 240 K, but not low or dramatically enough to indicate a phase transition. It may be that a potential collapse would have occurred at too high temperatures to be energetically favourable for this degeneracy. This phenomenon could have been investigated more thoroughly by running simulation on a number of degeneracies between 24 and 36 to establish an eventual cut-off point.

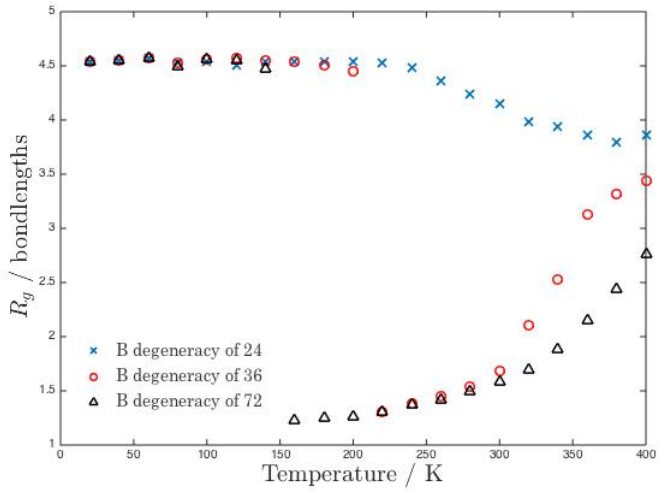

Figure 10: The average radius of gyration as a function of temperature for three degeneracies of state B; 24, 36 and 72.

4.2 Multiple-chain simulations

Simulations on systems with multiple chains also confirmed a sudden collapse of the polymers and an aggregation of the system both when increasing the temperature stepwise during the simulation and when simulating at multiple fixed temperatures, while the same was not observed when decreasing the temperature. At lower temperatures the chains were distributed evenly throughout the simulation box and the individual chains adopted a coil conformation. Most of the monomers were also in the hydrophilic state A. Then, passing over a certain temperature, all monomers in the system could be seen to collapse and aggregate in large clusters with an accompanying switch of most of the monomers to the hydrophobic state B. Figure 11 shows the polymer chains before and after the aggregation of the chains for simulations performed on chain-lengths of 20, 40 and 200 monomers.

Interestingly, all simulated multiple-chain systems aggregated, even the system with 20-monomer chains (as can be seen in figure 11b) which did not aggregate during the single-chain simulations. The only distinction between separate chains in the simulation program was the constraint of maintaining fixed bond lengths between neighbouring monomers. Since there was no difference in the interaction energies between monomers in different chains compared to those within the same chain, it is likely that during the simulation some of the 20-monomer chains came close enough to each other to no longer act as separate chains, and this would have caused an aggregation at temperatures around the observed phase transition for the other systems. This could perhaps have been confirmed by running simulations on a system with only two or three 20-monomer chains and by running simulations with varying densities on the 20-mer system.

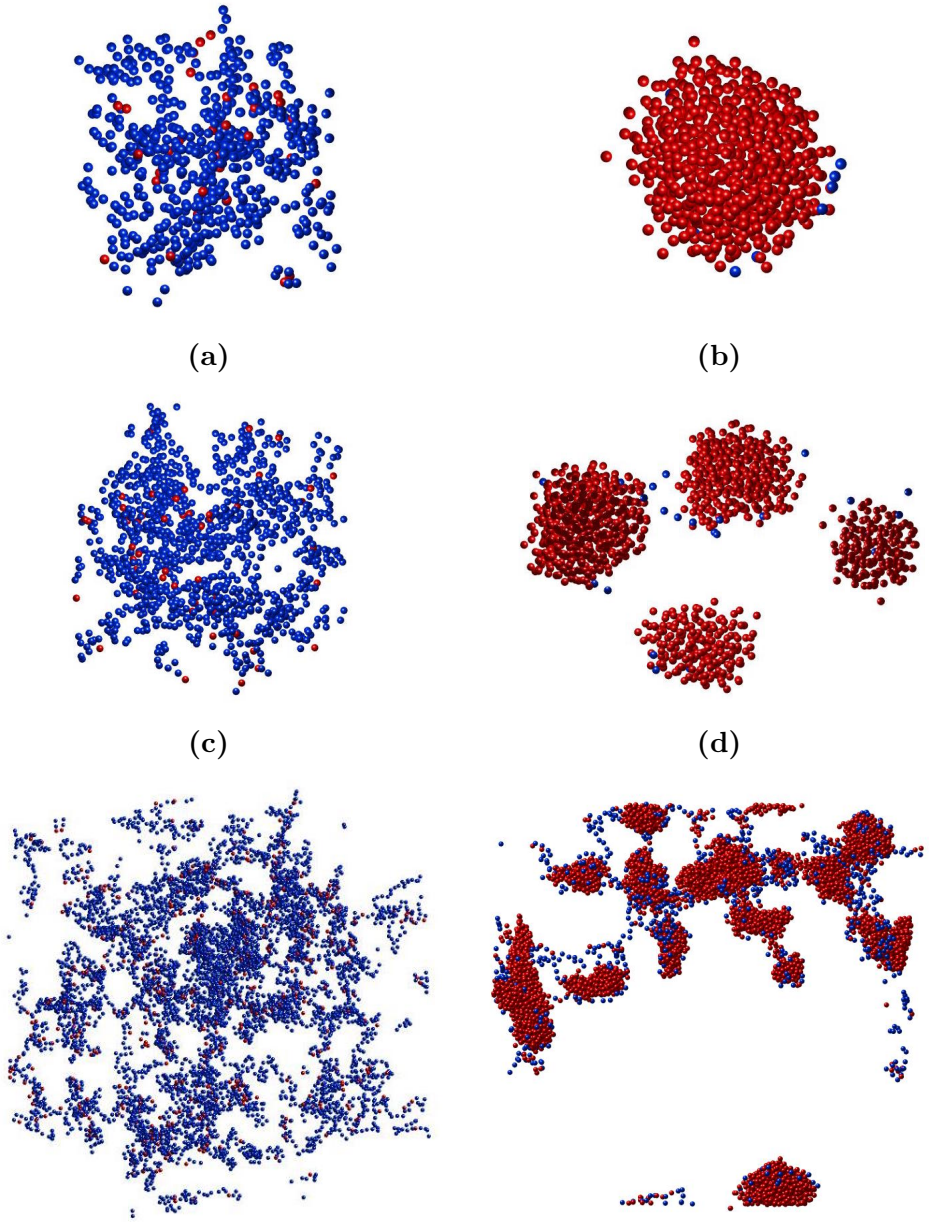

Figure 11: Snapshots from simulations of systems with multiple chains. The monomers of the polymer chains are displayed as spheres where monomers in state A are coloured blue and monomers in state B are coloured red. All systems consist of 30 chains, and the number of monomers per chain in each figure is 20 (a,b), 40 (c,d) and 200 (e,f). The figures on the left (a,c,e) show the chains before the phase transition and the figures on the right (b,d,f) the chains after the phase transition.

It can also be seen in figure 11 that while for the 20-monomer chains the aggregation produced one globule consisting of all chains, the simulations performed on 40-mer chains and over generally resulted in multiple compact clusters above the phase transition temperature. It is likely that these multiple clusters would have eventually aggregated given enough time or by moving the chains in other ways. Moves where an entire aggregated cluster would be identified and translated randomly, perhaps after noting a decrease in the acceptance rate of the Monte Carlo moves, could have been used to investigate this possibility.

4.2.1 Comparisons to the single-chain simulations

Because of the variation in the temperature of collapse for the single chain runs depending on the length of the simulations, a specific temperature for the collapse of the chain could not be determined. Thus, it could not be affirmed if the collapse of a single chain and the aggregation of a system of multiple chains occurred at the same temperature.

A slight variation in the temperature of aggregation was also observed in the multiple chain systems. However, due to the longer simulation time required for the multiple chain systems, this variation was only observed within a temperature span of 60 K. For simulations at fixed temperatures of 240 K and higher, signs of an aggregation appeared immediately after the simulation stated. This coincides with the results from the longer runs on fixed temperatures with a single polymer chain in figure 9a. Figure 9d, which shows the development of the radius of gyration during a simulation run at 240 K is the first temperature at which the collapse of the chain could be seen to be immediate during the single chain runs.

While a common temperature for a collapse could not be established, single polymer and multiple polymer systems thus behaved similarly; showing a collapse or aggregation upon increasing the temperature, and showing that the temperature of transition depended on the simulation time but not on the number of monomers in the polymer chains.

4.3 Improvements on the simulation program

Various improvements in the simulation programs could have been made to enhance the efficiency of the simulations. During the simulations, the acceptance rate of the trial moves could be seen to decrease drastically as the chains collapsed. This was especially true for the pivot move. An automatic adjustment of the maximum rotation angle or translation displacement as the acceptance rate dropped could have been used to improve the acceptance rate. Adjustable percentages of the probability of certain moves to be performed could also have been

implemented. This could have been used to decrease the probability of the pivot move to be performed when the chains had collapsed into globules.

As already mentioned, moves where entire clusters of polymer chains are moved could have been used for the multiple chain simulations. This would also have improved the acceptance rate for the simulations where the system aggregated, as the entanglement of the chains prevented single chains to be translated. The implementation of these types of moves would have to be restricted to systems where aggregation had been detected so as not to lead to an increase in computation time.

More time efficient methods of calculating the energy and distances between monomers could have been used. For the larger multiple-chain systems the efficiency could probably have been improved by using neighbour lists that kept track of monomers within the cut-off distance.

5 Conclusions

In conclusion, the model used in the simulations in this work can, with limitations, be used to explain the coil-to-globule transition in polymer solutions displaying a lower critical solution temperature. The discrepancies between simulations performed by increasing versus decreasing the temperature of the system should be investigated more thoroughly. It was also shown that there is a link between the collapse of a single polymer chain and the aggregation of a system with multiple chains. However, due to variations in the phase transition temperature depending on the starting point and length of the simulations for both the single-chain and multiple-chain simulations, an exact temperature for the phase transitions could not be determined.

Acknowledgements

First and foremost, I would like to thank my supervisor Jan Forsman for his helpful guidance throughout this entire project. I also thank Hongduo Lu for setting me on a wonderful starting point with her clear and pedagogical explanations of the simulation method, Maria Jansson for her help with various miscellaneous problems, Per-Olof Widmark for his work as my examiner and Marie Skepö for taking me on initially and welcoming me into her group. Lastly I would like to thank everyone on the third floor for their welcoming and kind treatment of me despite my somewhat antisocial tendencies.

References

[1] Ward, M. A.; Georgiou, T. K. Thermoresponsive Polymers for Biomedical Applications. *Polymers* **2011,** *3,* 1215-1242.

[2] Hamley, I. W. *Introduction to Soft Matter;* John Wiley & Sons Ltd.: Chichester, England, 2000; pp 41-43, 53-58, 74-90.

[3] Li, P.; Zhang, Z.; Su, Z.; Wei, G. Thermosensitive polymeric micelles based on the triblock copolymer poly(D,L-lactide)-*b*-poly(*N*-isopropyl acrylamide)-*b*-poly(D,L-lactide) for controllable drug delivery. *J. Appl. Polym. Sci.* **2017,** *134,* 45304.

[4] Wang, W.; Deng, L.; Liu, S.; Li, X.; Zhao, X.; Hu, R.; Zhang, J.; Han, H.; Dong, A. Adjustable degradation and drug release of a thermosensitive hydrogel based on a pendant cyclic ether modified poly(ε-caprolactone) and poly(ethylene glycol)co-polymer. *Acta Biomaterialia* **2012,** *8,* 3963-3978.

[5] Jiang, G.; Sun, J.; Ding, F. PEG-g-chitosan thermosensitive hydrogel for implant drug delivery: cytotoxicity, in vivo degradation and drug release. *J. Biomater. Sci. Polymer Edn.* **2014,** *25,* 241-256.

[6] Allen, A. C. B.; Barone, E.; O'Keefe Crosby, C.; Suggs, L. J.; Zoldan, J. Electrospun poly(*N*-isopropyl acrylamide)/poly(captolactone) fibers for the generation of anisotropic cell sheets. *Biomater. Sci.* **2017,** *5,* 1661.

[7] Sakuma, M.; Kumashiro, Y.; Nakayama, M.; Tanaka, N.; Haruguchi, Y.; Umemura, K.; Shimizu, T.; Yamato, M.; Okano, T. Preparation of Thermoresponsive Nanostructured Surfaces for Tissue Engineering. *J. Vis. Exp.* **2016,** *109,* 53465.

[8] Yoon, J.; Park, K.; Song, S. A thermosensitive poly(organophosphazene) hydrogel for injectable tissue-engineering applications. *J. Biomater. Sci. Polymer Edn.* **2007,** *18,* 1181-1193.

[9] Bharadwaj, S.; Kumar, P. B. S.; Komura, S.; Deshpande, A. P. Spherically Symmetric Solvent is Sufficient to Explain the LCST Mechanism in Polymer Solutions. *Macromol. Theory Simul.* **2017,** *26,* 1600073.

[10] de Oliveira, T. E.; Mukherji, D.; Kremer, K.; Netz, P. A. Effect of stereochemistry and copolymerization on the LCST of PNIPAm. *J. Chem. Phys.* **2017,** *146,* 034904.

[11] Ortiz-Estrada, C. H.; Luna-Bárcenas, G.; Alvarado, F. J.; Gonzales-Alatorre, G.; Sanchez, I. C.; Castillo-Tejas, J.; Manero-Brito, O.; Ramírez, N. F.; García, S. R. V. Polymer Chain Collapse in Supercritical Fluids. 1. Molecular Simulation Results. *Macromol. Symp.* **2009,** *283-284,* 250-265.

[12] de Oliveira, T. E.; Marques, C. M.; Netz, P. A. Molecular dynamics study of the LCST transition in aqueous poly(*N*-*n*-propylacrylamide). *Phys. Chem. Chem. Phys.* **2018,** *20,* 10100.

[13] Karlström, G. A. A New Model for Upper and Lower Critical Solution Temperatures in Poly(ethylene oxide) Solutions. *J. Phys. Chem.* **1985,** *89,* 4962-4964.

[14] Murrell, J. N.; Boucher, E. A. *Properties of liquids and solutions;* John Wiley & Sons Ltd.: Chichester, England, 1982; pp 31-34, 52-58, 243-244.

[15] Leach, A. R. *Molecular Modelling: Principles and Applications,* 2nd ed.; Pearson Education Limited: Harlow, England, 2001; pp 303, 306-307, 317-319.

[16] Metropolis, N.; Rosenbluth, A. W.; Rosenbluth, M. N.; Teller, A. H.; Teller, E. Equation of State Calculations by Fast Computing Machines. *J. Chem. Phys.* **1953,** *21,* 1087-1092.

[17] Allen, M. P.; Tildesley, D. J. *Computer Simulation of Liquids;* Oxford University Press: Oxford, England, 1987; pp 6-12, 23-25.

[18] Xie, F.; Woodward, C. E.; Forsman, J. Fluid-Fluid Transitions at Bulk Supercritical Conditions. *Langmuir,* **2013,** *29,* 2659-2666.

[19] Xie, F.; Woodward, C. E.; Forsman, J. Non-monotonic temperature response of polymer mediated interactions. *Soft Matter,* **2016,** *12,* 658.

[20] Xie, F.; Woodward, C. E.; Forsman, J. Theoretical Predictions of Temperature-Induced Gelation in Aqueous Dispersions Containing PEO-Grafted Particles. *J. Phys. Chem.* **2016,** *120,* 3969-3977.